


# The legacy of water deficit on populations having experienced negative hydraulic safety margin

Marta Benito Garzón<sup>1\*</sup>  | Noelia González Muñoz<sup>1\*</sup> | Jean-Pierre Wigneron<sup>2</sup> |  
Christophe Moisy<sup>2</sup> | Juan Fernández-Manjarrés<sup>3</sup> | Sylvain Delzon<sup>1</sup>

<sup>1</sup>BIOGECO, INRA, University of Bordeaux, Pessac, France

<sup>2</sup>UR1263 ISPA, Villenave d'Ornon, France

<sup>3</sup>CNRS, Laboratoire Ecologie, Systématique Evolution, Université Paris-Sud, Orsay Cedex, France

## Correspondence

Marta Benito Garzón, BIOGECO, INRA, University of Bordeaux, Bat B2, Allée Geoffroy-St-Hilaire, CS50023, 33615 Pessac, France.  
Email: marta.benito-garzon@inra.fr

## Funding information

Investments for the Future IDEX Bordeaux, Grant/Award Number: ANR-10-IDEX-03-02; EQUIPEX, Grant/Award Number: ANR-10-EQPX-16 and XYLOFOREST; Agreenskills; EU's Seventh Framework Programme, Grant/Award Number: FP7-26719

Editor: Greg Jordan

## Abstract

**Aim:** The aim was to examine whether recent mortality can be explained by hydraulic failure linked to water deficit.

**Location:** Western Europe.

**Time period:** 1986–2014.

**Major taxa studied:** Forty-four tree species.

**Methods:** We modelled the hydraulic safety margin (HSM) across the ranges of 44 tree species at their driest margin ( $n = 193,261$  plots), defined as the difference between the estimated minimal soil water potential of each plot and the species water stress threshold, which corresponds to the hydraulic failure of the vascular system. Soil water potential was estimated by applying Campbell's equations on the minimal and maximal soil water contents estimated from 1979 to 2010 in the top 289 cm of soil and five soil textures across the species ranges. For each species, we modelled the amount of average mortality derived from plots of the Spanish and French National Forest Inventories to the variation in modelled hydraulic safety margin and environmental drivers across the species ranges using hurdle models.

**Results:** We did not identify any global convergence of modelled HSM within the species distribution ranges, finding instead a rather large variability in modelled HSM for most of the studied species. Fifteen species, out of 25 for which the models were practicable, showed significantly higher mortality in populations with negative HSM in comparison to those showing positive HSM, with positive and negative interaction along the aridity index.

**Main conclusions:** The combination of competition, average climate and modelled HSM explained average tree mortality. Most of the species presented at least one population that had already experienced a negative HSM and many other populations a positive but narrow HSM, suggesting that climate change is likely to push some populations towards a higher risk of hydraulic failure in the drier conditions projected for Western Europe.

## KEYWORDS

drier edge, mortality, national forest inventories, resistance to embolism, soil water content, soil water potential, Western Europe

\*These authors contributed equally to this study.

## 1 | INTRODUCTION

The number of forest mortality events has increased in recent decades in some regions (Peng et al., 2011; Phillips et al., 2009; van Mantgem et al., 2009), making ecological research on tree mortality a priority (Bonan, 2008). However, attention has mainly focused on mortality die-back (Allen, Breshears, & McDowell, 2010; Allen et al., 2015; Anderegg et al., 2016), and little is known about the increase in average mortality along large climatic gradients (Berdanier & Clark, 2016; Clark, Iverson, & Woodall, 2016; Hartmann, Adams, Anderegg, Jansen, & Zeppel, 2015; Neumann, Mues, Moreno, Hasenauer, & Seidl, 2017; Young et al., 2017). Explaining these patterns in forest vulnerability is challenging because tree mortality depends on the ecophysiological limits of each individual species and the interactions with other species, which can change along species ranges (Benito-Garzón, Ruiz-Benito, & Zavala, 2013; Gómez-Aparicio, García-Valdés, Ruiz-Benito, & Zavala, 2011; Kunstler et al., 2016; Ruiz-Benito, Lines, Gómez-Aparicio, Zavala, & Coomes, 2013). Moreover, the link between hydraulic traits and mortality across species ranges has not generally been included in vegetation models (Anderegg, Flint, & Huang, 2015), which could lead to incorrect interpretations of the effects of climate change on trees inhabiting ranges affected by very different environments. Hence, attributing average tree mortality to water stress at large scales remains a challenge (Clark et al., 2016; Steinkamp & Hickler, 2015; Young et al., 2017), and there is an urgent need to couple the physiological margin of drought tolerance of species along climatic gradients to understand vegetation patterns at large scales.

Large variations in mortality rates have been observed across species ranges (Benito-Garzón et al., 2013; Kunstler et al., 2016; Purves, 2009; Vanderwel, Lyutsarev, & Purves, 2013), suggesting that this variability is mostly driven by climatic gradients (Neumann et al., 2017; Young et al., 2017). The relationship between mortality and climate is so strong that it can delimit the ranges of species, in particular at the drier edge of the distribution (Benito-Garzón et al., 2013; Kunstler et al., 2016; Purves, 2009; Stahl, Reu, & Wirth, 2014). For instance, in Western Europe, the drier edge of temperate tree species is mostly occupied by populations showing high mortality and low reproductive rates and biomass, indicating a retraction of their current distribution, which reflects the current pattern of climate change (Benito-Garzón et al., 2013; Linares & Camarero, 2011; Urli et al., 2015). Furthermore, it remains unexplored whether the mortality patterns at the drier edge of the species distributions are attributable to climate that makes species reach their ecophysiological limit at that point. In this sense, the inclusion of hydraulic traits explaining mortality along the species ranges would make a major contribution to the interpretation of the effects of climate change on trees growing in very different environments across their distribution ranges. Nonetheless, studies linking patterns of mortality and hydraulic traits are scarce, and most of them have been carried out in laboratory conditions for a few species (David-Schwartz et al., 2016; López, Cano, Choat, Cochard, & Gil, 2016; López et al., 2013; but see Anderegg et al., 2016).

The extent to which hydraulic failure and carbon starvation can explain tree mortality can potentially be related to the intensity and

duration of water stress (McDowell et al., 2008). Recent studies have shown that trees subjected to drought die sooner than starved trees (Hartmann, Ziegler, Kolle, & Trumbore, 2013) and that tree mortality can be predicted exclusively from the loss of vascular transport capacity (Anderegg et al., 2015). Indeed, hydraulic failure of the vascular system has been shown to be linked closely to survival in extreme drought conditions in both conifers and angiosperms (Brodribb & Cochard, 2009; Brodribb, Bowman, Nichols, Delzon, & Burrett, 2010; Urli et al., 2013). Hydraulic failure occurs when plant water potential drops sufficiently to provoke air embolisms that block xylem vessels, reducing the ability of trees to move water from the soil to their leaves (Tyree, 1999). Embolism in the xylem vessels can potentially lead to a decrease in the total volume of trees by branch reduction or even tree death (Brodribb & Hill, 1999; Brodribb et al., 2010; Lens et al., 2013; Urli et al., 2013). The loss of conductivity that provokes hydraulic failure has been suggested to be at 50% for gymnosperms ( $\Psi_{50}$ ) and at 88% for angiosperms ( $\Psi_{88}$ ). Resistance to embolism varies among species and biomes (Maherali, Pockman, & Jackson, 2004), and in general, species inhabiting drier environments show a greater resistance to embolism than those in wetter ones (Choat, Jansen, & Brodribb, 2012). Less is known about the intraspecific variability of resistance to embolism; whereas low variation has been measured for some species (Lamy et al., 2014; Martínez-Vilalta et al., 2009; Sáenz-Romero et al., 2013; Wortemann et al., 2011), other species do show variability in resistance to embolism (David-Schwartz et al., 2016; López et al., 2016). However, for most species, the intraspecific variation in the resistance to embolism is still unknown.

Most tree species seem to operate very close to their hydraulic failure level (i.e., they have a narrow hydraulic safety margin; Choat et al., 2012), and thus appear to be highly vulnerable to drought-induced mortality when conditions become warmer and/or drier (Engelbrecht, 2012). The hydraulic safety margin (HSM) corresponds to the difference between the minimal water potential experienced by the species in natural conditions ( $\Psi_i$ ) and the water potential at which the loss of vascular conductivity provokes hydraulic failure (Meinzer, Johnson, Lachenbruch, McCulloh, & Woodruff, 2009). Although it is known that tree species currently survive within typically small safety margins (Choat et al., 2012) and that vulnerability to embolism and the hydraulic safety margin are important predictors of cross-species mortality at global scales (Anderegg et al., 2016), the within-species range variation in hydraulic safety margin and its potential relationship with tree mortality remain completely unknown.

Here, we hypothesize that the footprint of drought linked to the species resistance to xylem embolism can already be observed in average mortality rates across large climatic gradients within species ranges. We therefore investigated the legacy of water deficit by comparing observed mortality in populations having experienced negative and positive hydraulic safety margins, in particular at the drier edge of species ranges. To achieve our aim, we combined spatial information of modelled soil water potential from climate data and soil texture maps with average mortality from 193,261 plots belonging to 44 species recorded in the French and Spanish National Forest Inventories (NFIs) with the species' threshold of hydraulic failure measured in laboratory

conditions ( $\Psi_{50/88}$ ). For spatial assessment of the modelled hydraulic safety margin across the distribution range of the 44 European species, we estimated for each NFI plot (population) the minimal soil water potential based on the texture of the soil and the soil volumetric water content of the last 30 years estimated at a depth of 289 cm. Finally, we tested the effect of hydraulic safety margin together with climatic factors and competition on the average tree mortality of the 44 species. Using this approach, we were able to identify those populations of each species that have operated with a negative hydraulic safety margin over the last 30 years and the relative effect of the modelled hydraulic safety margin in average mortality. To the best of our knowledge, our results report, for the first time, the relationship between the modelled hydraulic safety margin and the water deficit legacy in the mortality of tree populations within species ranges, providing useful information to identify potential shifts in European species distribution and composition attributable to ongoing climate change.

## 2 | MATERIALS AND METHODS

### 2.1 | Mortality estimation from national forest inventories

Mortality was estimated for each of the 44 species presented in the French and Spanish National Forest Inventories at the plot level (NFIs; Supporting Information Table S1). The sampling for the Spanish NFI was conducted from 1986 to 1996 (second campaign) and from 1997 to 2007 (third campaign), and mortality was recorded as the number of trees found dead in the third campaign that were alive during the second one. The sampling for the French NFI was conducted from 2005 to 2014, and mortality was recorded for adult trees that died up to 5 years before the records were made. Plots for both NFIs are circular, with a radius of 25 m. Mortality was estimated as the number of dead trees of a given species per plot (Benito-Garzón & Fernandez-Manjarrés, 2015). Managed plots were filtered out from the final database.

The NFI plots were also used to define the distribution of the 44 species considered (Supporting Information Figure S1). For simplicity, we use the term 'populations' to refer to the plots recorded in the NFIs. Potential competition was calculated as the sum of the basal area of tree neighbours in the plot.

### 2.2 | Determination of the species' threshold of hydraulic failure

For conifers, resistance to embolism was determined in the Cavitplace platform (University of Bordeaux, Talence, France; <http://sylvain-delzon.com/caviplace>). One to two branches were collected from an average of five to 10 healthy trees per species in Kew Gardens (Royal Botanic Gardens) or at the Bordeaux Botanical garden (Talence, France; for more details, see Bouche, Larter, & Domec, 2014). After harvesting, leaves or needles were immediately removed, and the branches were wrapped in moist paper towel, placed in black bags and immediately sent to the laboratory. The branches were kept wet and cool (3 °C) until embolism resistance was measured [at a maximum of 3 weeks

after their collection, and no change in vulnerability to embolism has been detected over 10 weeks (Herbette et al., 2010)]. Before measurement, the bark was removed and the branches were recut with a razor blade underwater to a standard length of 0.27 m. In the Cavitron method, a centrifugal force is applied to induce a loss of conductance by embolism, simulating a water stress-induced embolism. To do this, the samples are inserted into a custom-built rotor (Precis 2000, Bordeaux, France) mounted on a high-speed centrifuge (Sorvall RC5, USA). Conductance measurements were taken using the Cavisoft software (version 2.0; BIOGECO, University of Bordeaux).

The xylem pressure ( $\Psi_i$ ) and percentage loss of conductance (PLC) were determined at different speeds, to obtain a vulnerability curve per sample (VC; i.e., percentage loss of xylem conductance as a function of xylem pressure; for details, see Delzon, Douthe, Sala, & Cochard, 2010).

For each sample, a sigmoid function (Pammenter & Vander Willigen, 1998) is fitted to the VC (proc NLIN, SAS version 9.2; SAS Institute, Cary, NC, USA) using the following equation:

$$PLC = \frac{100}{1 + \exp\left(\frac{S}{\Psi_i - \Psi_{50}}\right)},$$

where  $\Psi_{50}$  (in megapascals) is the xylem pressure inducing 50% loss of conductance, and  $S$  (expressed as a percentage per megapascal) is the slope of the vulnerability curve at the inflexion point. The xylem pressure inducing 88% of PLC ( $\Psi_{88}$ , in megapascals) was calculated from the equation of Domec and Gartner (2001):

$$\Psi_{88} = -50/S + \Psi_{50}.$$

For angiosperms, we used a previously reported dataset (Lens, Picon-Cochard, & Delmas, 2016), in which sigmoidal vulnerability curves were kept only to avoid bias attributable to open vessel artefacts. Recent direct observations of embolism formation by X-ray tomography confirmed the reliability of these values (Choat et al., 2016; Cochard, Delzon, & Badel, 2015; Cochard et al., 2013; Torres-Ruiz et al., 2014, 2017).

### 2.3 | Environmental data: average climate, volumetric soil water content and soil texture

We used gridded average climate from 1960 to 1990 at 1 km resolution (Hijmans, Cameron, Parra, Jones, & Jarvis, 2005) for six climatic variables related to mortality: mean annual temperature (BIO1), maximum temperature of the warmest month (BIO5), minimum temperature of the coldest month (BIO6), precipitation of the wettest month (BIO13), precipitation of the driest month (BIO14) and annual precipitation (BIO12) (<http://www.worldclim.org/>). We also used the aridity index (AI) at 1 km resolution, estimated as mean annual precipitation/mean annual potential evapotranspiration, as obtained from <http://www.cgiar-csi.org/>.

Minimum and maximum monthly volumetric soil water contents from 1979 to 2010 were estimated from the ERA-INTERIM daily global atmospheric reanalysis database (Dee et al., 2011; <http://apps.ecmwf.int/datasets/>) from the soil surface to a depth of 289 cm at T255 spectral spatial resolution (Balsamo et al., 2015). We used a gridded dataset

at a spatial resolution of  $0.125^\circ$  (c.  $10 \text{ km} \times 14 \text{ km}$  at a latitude of  $45^\circ$ ). The minimum ( $W_i$ ) and maximum ( $W_s$ ) monthly volumetric soil water contents were calculated as the monthly average water content values for the 5 years showing the lowest and highest values of volumetric soil water from 1979 to 2010, respectively. We extracted the dominant surface textural classes from the European Soil Database at a resolution of  $1 \text{ km}$  (Panagos, Van Liedekerke, Jones, & Montarella, 2012; <http://eusoils.jrc.ec.europa.eu/wrb/>). Dominant surface textural classes were used to downscale the ERA-INTERIM resolution to calculate the soil-related characteristics from Campbell's equations at  $1 \text{ km}$  resolution (Campbell, 1985; see "2.4. Modelling soil water potential" section below). The dominant surface textural soils were aggregated into five texture classes to fit Campbell's equations: coarse, medium, medium fine, fine and very fine (Supporting Information Table S1).

## 2.4 | Modelling soil water potential

For each NFI plot, we equalized the maximum volumetric soil water content from 1979 to 2010 ( $W_s$ ), as explained above, to the total saturation of the soil at which the soil water potential (SWP) is zero. This allowed us to calculate the soil water potential for each of the five soil types considered (see Supporting Information Table S1, showing the soil water potential of soil types) following Campbell's equations (Campbell, 1985; Sperry, Adler, Campbell, & Comstock, 1998).

Campbell's equations were used to model the minimum soil water potential ( $\Psi_i$ ) from the values of the minimum soil water content ( $W_i$ ) that were obtained from the ERA-INTERIM dataset. More specifically,  $W_i$  can be computed as a function of  $\Psi_i$  and the water content ( $W_e$ ) and water potential ( $\Psi_e$ ) at maximum hydration.

$$W_i = W_s (\Psi_e / \Psi_i)^{-1/b}.$$

Then,  $\Psi_i$  is estimated as:

$$\Psi_i = \Psi_e (W_i / W_s)^b,$$

where  $W_s$  is the maximum water content and  $W_i$  the minimum water content, as explained above. The parameters  $b$  and  $\Psi_e$  are functions of the soil texture (Campbell, 1985), as follows:

$$\Psi_e = -0.5 \times \text{GMD}^{-0.5}$$

$$b = -2\Psi_e + 0.2\text{GSD},$$

where GMD is the geometric particle diameter, and GSD is the geometric standard deviation of particle size (in millimetres) for each type of soil defined above (Supporting Information Table S1).

This allowed us to obtain one  $\Psi_i$  value per NFI plot. For analysis at the species level, we modelled the minimum soil water potential within each species range ( $\Psi_{\min}$ ) as the average of the  $\Psi_i$  values in the driest quartile of the species distribution. We worked on the driest margin of the species distribution to evaluate the effect of large water deficit on mortality. Depending on the species,  $\Psi_{\min}$  varies between  $-1.822$  and  $-12 \text{ MPa}$  in the top  $289 \text{ cm}$  of soil, which overlaps with the  $\Psi_{50/88}$  of the 44 species analysed (Supporting Information Table S2). Among the different soil types, loam soils showed the highest minimum water volumetric content for a certain soil water potential (Supporting Information Figure S1).

## 2.5 | Hydraulic safety margin within species ranges

Hydraulic safety margins (HSMs) are typically defined as the difference between the minimum midday water potential measured in natural conditions ( $\Psi_i$ ) and the water potential inducing 12, 50 or 88% of embolism (Choat et al., 2012; Delzon & Cochard, 2014; Meinzer et al., 2009). From an ecological perspective, it is relevant to define hydraulic safety margins as a threshold for tree mortality. In conifers, the lethal level of embolism was found to be close to 50% of embolized conduits in stems (Brodribb & Cochard, 2009; Brodribb et al., 2010; Uri et al., 2013), whereas for angiosperms, the threshold of hydraulic failure is closer to 88% (Barigah, Charrier, & Douris, 2013; Uri et al., 2013). We therefore used  $\Psi_{50}$  and  $\Psi_{88}$  as thresholds of tree mortality ( $\Psi_{50/88}$ ) for conifers and angiosperms, respectively.

We calculated the HSM at the species and population (NFI plot) levels. At the species level, HSM was calculated as the difference between the modelled soil water potential (with the assumption that, during extreme drought, stomata are closed and there is no water flow, hence soil water potential is equal to the stem water potential) at the lowest quartile of the distribution of the species ( $\Psi_{\min}$ ) and the specific  $\Psi_{50/88}$ :

$$\text{HSM} = \Psi_{\min} - \Psi_{50/88}.$$

To calculate the modelled HSM at the population level, we assumed that the water potential measured in plants in natural conditions ( $\Psi_i$ ) can be equated to that of the soil (SWP). To test this assumption, we conducted Spearman's correlation analyses between the average  $\Psi_{50/88}$  of the 44 species (angiosperms and gymnosperms together and separately; Supporting Information Table S2) and the estimated soil water potential at the lowest quartile ( $\Psi_{\min}$ ) of each species distribution range. If this condition was fulfilled across species, then the populations having experienced positive and negative modelled HSM of the species could be identified and mapped. The modelled HSM at the population level was then calculated by applying an equation similar to that at the species level, but to each plot across the distribution range of each of the 44 species:

$$\text{HSM} = \Psi_i - \Psi_{50/88},$$

where  $\Psi_i$  is the soil water potential calculated for each plot as, explained above (see section 2.4 Modelling soil water potential), and  $\Psi_{50/88}$  is the point of critical loss of conductivity for each species. In other words, when modelled HSM is zero,  $\Psi_i$  is equal to  $\Psi_{50/88}$ .

Negative values of modelled HSM identify those populations present at geographical locations at which the modelled SWP is more negative than the  $\Psi_{50/88}$  of the species, meaning that these populations have operated outside their hydraulic safety margin over the last 30 years.

## 2.6 | The legacy of water deficit in mortality of populations with negative hydraulic safety margin

The variation of modelled SWP within the species ranges in combination with the specific  $\Psi_{50/88}$  allowed us to identify those populations with negative and positive modelled HSM across the distribution



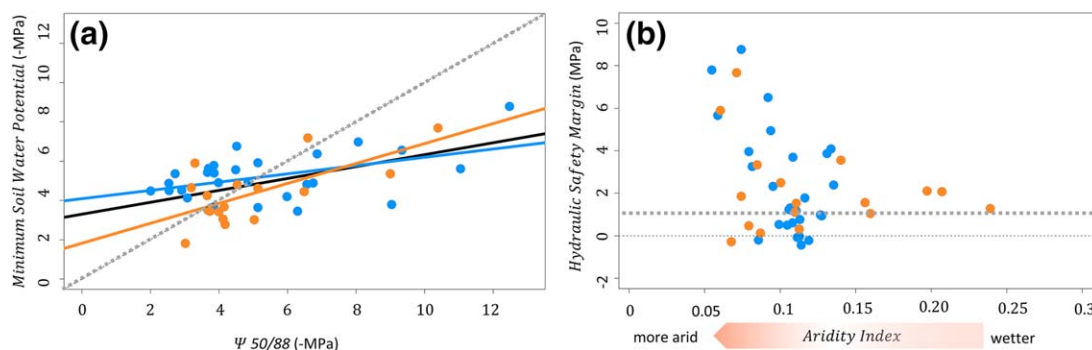


**FIGURE 1** (a) Significant correlations between the soil water potential modelled at the driest quartile of each species distribution ( $\Psi_i$ ) and the water potential inducing 50 or 88% of xylem embolism,  $\Psi_{50/88}$  ( $\Psi_{50}$  and  $\Psi_{88}$ , for gymnosperms and angiosperms, respectively) per species, when considering gymnosperm (blue;  $\rho = 0.679$ ,  $p = .003$ ) and angiosperm (orange;  $\rho = 0.475$ ,  $p = .034$ ) species separately and for both conifers and angiosperms considered together (black;  $\rho = 0.533$ ,  $p < .001$ ). The dotted line represents the hydraulic safety margin (HSM), which at the species level was calculated as  $\Psi_i - \Psi_{50/88}$ . (b) Modelled hydraulic safety margin versus the aridity index (mean annual precipitation/mean potential evapotranspiration) measured at the lowest quartile of the species ranges. Again, gymnosperms and angiosperms are represented in blue and orange, respectively. The dotted line represents the hydraulic safety margin when the minimum soil water potential ( $\Psi_i$ ) equals the  $\Psi_{50/88}$  ( $\Psi_{50}$  and  $\Psi_{88}$  for gymnosperms and angiosperms, respectively)

ranges of the species. The rationale behind this is that populations with modelled SWP lower than the specific  $\Psi_{50/88}$  have experienced negative modelled HSM at some stage during the last 30 years, which could have left a mark in their average mortality. We define the legacy of water deficit in a given population when mortality was significantly higher in populations with negative modelled HSM than in those with positive modelled HSM.

## 2.7 | Statistical analysis

To understand the main possible climatic drivers of tree mortality across the species ranges, and because mortality has a multifactorial origin and hydraulic failure is considered to shape the driest part of the species distributions, we considered in our models seven climatic drivers (BIO1, BIO5, BIO6, BIO12, BIO13, BIO14 and the aridity index) and competition (calculated as the sum of the basal area of neighbouring trees in each plot).

To handle the zero-inflated distribution of mortality, we built hurdle models (*pscl* R library), which allowed us to model the occurrence of mortality (yes/no states) and the amount of mortality as separate processes (Young et al., 2017). In hurdle models, the occurrence of mortality is estimated firstly by binomial models with logarithmic transformation, and the amount of predicted mortality is estimated secondly by negative binomial models with logarithmic transformation. The goodness of fit is estimated with the area under the curve (AUC) and the pseudo- $R^2$ . Within these two separate models, we used the second one to explain the amount of mortality across aridity gradients for populations located at the most negative quartile of the modelled HSM, at the most positive quartile of the modelled HSM and for populations with average values of modelled HSM within each species' ranges.

Hence, a hurdle model was performed for each species to test the combined effects of competition, hydraulic safety margin, aridity and average climate effects on average tree mortality per plot (i.e., the percentage of dead trees of a given species per plot), and special attention

was paid to the model explaining the amount of mortality found per plot. The interactions between modelled HSM and aridity, and the modelled HSM and plot competition were also considered in the model as explanatory factors. Owing to the small number of trees recorded in NFIs for some species and/or to the lack of model convergence for others, hurdle models were finally calculated for 25 tree species. All calculations were performed with the software R Project for Statistical Computing (R Development Core Team, 2016).

## 3 | RESULTS

### 3.1 | Correlation between species' hydraulic threshold and minimal soil water potential

We found a significant and positive correlation between the modelled SWP measured at the driest quartile of the species distribution ( $\Psi_{\min}$ ) and the species hydraulic threshold ( $\Psi_{50/88}$ ;  $\rho = .533$ ,  $p < .001$ ). This relationship held even when considering angiosperm ( $\rho = .475$ ,  $p = .034$ ) and gymnosperm species ( $\rho = .679$ ,  $p = .003$ ) separately. The  $\Psi_{\min}$  ranged between  $-1.82$  and  $-8.79$  MPa, whereas  $\Psi_{50/88}$  varied from  $-2$  to  $-12.48$  MPa for the species studied. Figure 1a shows that species more resistant to embolism (more negative  $\Psi_{50/88}$ ) experience more negative soil water potentials and therefore inhabit more arid environments. Likewise, species with higher hydraulic safety margins inhabit drier environments (Figure 1b). This correlation was significant for angiosperms ( $\rho = -.550$ ,  $p = .002$ ) and when all species were considered together ( $\rho = -.310$ ,  $p = .037$ ), but not for gymnosperms alone ( $\rho = -.220$ ,  $p = .402$ ).

### 3.2 | How variable is the hydraulic safety margin within species?

Within-species variability in modelled hydraulic safety margin was large for all of the species, except for *Pinus cembra* and *Abies pinsapo*, which were also the only species without populations having experienced

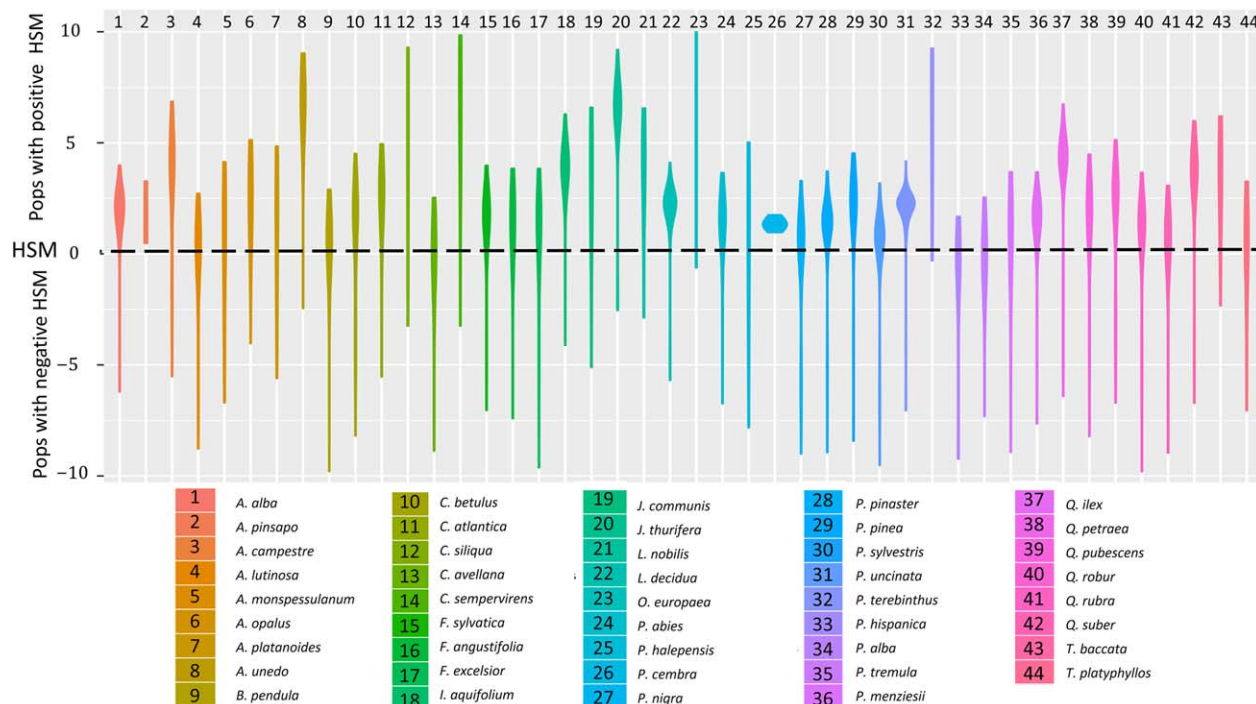


**FIGURE 2** Modelled hydraulic safety margin (HSM) across the distribution range of the 44 study species. At the population level, HSM was modelled as the difference in soil water potential in each National Forest Inventory plot and the specific tree mortality threshold,  $\Psi_{50}$  and  $\Psi_{88}$  for gymnosperms and angiosperms, respectively. The different colours and numbers represent the different species, following the same order as in the figure legend. Violin plots illustrate a compact display of a continuous distribution

negative modelled HSM (Figure 2; Supporting Information Table S2). Indeed, on average, more than one-third of the populations of each studied species have operated with negative hydraulic safety ranges (NFI plots; Supporting Information Table S2), except *Platanus hispanica* and *Populus alba*, for which 70 and 52% of their populations have operated with negative modelled HSM, respectively.

### 3.3 | Combined effects of hydraulic safety margin, competition and climate on tree mortality across species ranges

Hurdle models separated mortality processes in the prediction of the occurrence of mortality (binomial model) and the prediction of probability of the specific amount of mortality per plot (negative binomial model). Here, the binomial and negative binomial models showed a goodness of fit (measured by the AUC and the  $R^2$ , respectively) ranging from zero (*Acer opalus*) to .88 (*Ilex aquifolium*) and from .08 (*Betula pendula*) to .96 (*I. aquifolium*), respectively (Supporting Information Table S3).

Climate and competition had a strong effect on both occurrence and probability of mortality (Supporting Information Table S3). The effect of competition on predicted occurrence of mortality was significant for all species except *I. aquifolium* and *Quercus suber* (Supporting Information Table S3), whereas the effect of competition on the probability of mortality was significant for all species but *I. aquifolium* (Supporting Information Table S3). The interaction between modelled HSM and competition was significant for most of the species for both the binomial and negative binomial models (Supporting Information Table S3).

For binomial models, modelled HSM or the statistical interaction between modelled HSM and aridity had a significant effect on the occurrence of mortality for all species except *A. opalus*, *B. pendula*, *Fraxinus excelsior*, *Quercus petraea* and *Q. suber* (Supporting Information Table S3).

Within hurdle models, we used the outputs of negative binomial mortality models that predict the probability of the specific amount of mortality per plot. We found a significant effect of the modelled HSM and/or the interaction of modelled HSM with aridity in the predicted amount of mortality in 21 out of the 25 study species (Supporting Information Table S3). Among them, 15 species showed higher probability of mortality for populations located at the more negative quartile of modelled HSM than those located at the more positive quartile or those having an average modelled HSM (namely, *Acer campestre*, *Alnus glutinosa*, *B. pendula*, *Corylus avellana*, *Carpinus betulus*, *F. excelsior*, *Larix decidua*, *Picea abies*, *Pinus halepensis*, *Pinus sylvestris*, *Pseudotsuga menziesii*, *Pinus uncinata*, *Q. petraea*, *Quercus pubescens*, *Quercus robur* and *Q. suber*; Supporting Information Table S3).

For some species, predicted mortality increases with aridity (*Abies alba*, *A. campestre*, *F. excelsior*, *L. decidua*, *P. halepensis*, *P. menziesii*, *Quercus ilex*, *Q. petraea* and *Q. pubescens*), whereas for other species the opposite pattern was found (*A. glutinosa*, *A. opalus*, *B. pendula*, *C. avellana*, *C. betulus*, *Fraxinus angustifolia*, *P. abies*, *Pinus pinaster*, *P. sylvestris*, *Q. robur* and *Q. suber*; Figure 3). More specifically, having negative HSM increases mortality particularly in arid environments in the cases of *B. pendula*, *C. avellana*, *P. abies*, *P. sylvestris* and *Q. suber*.

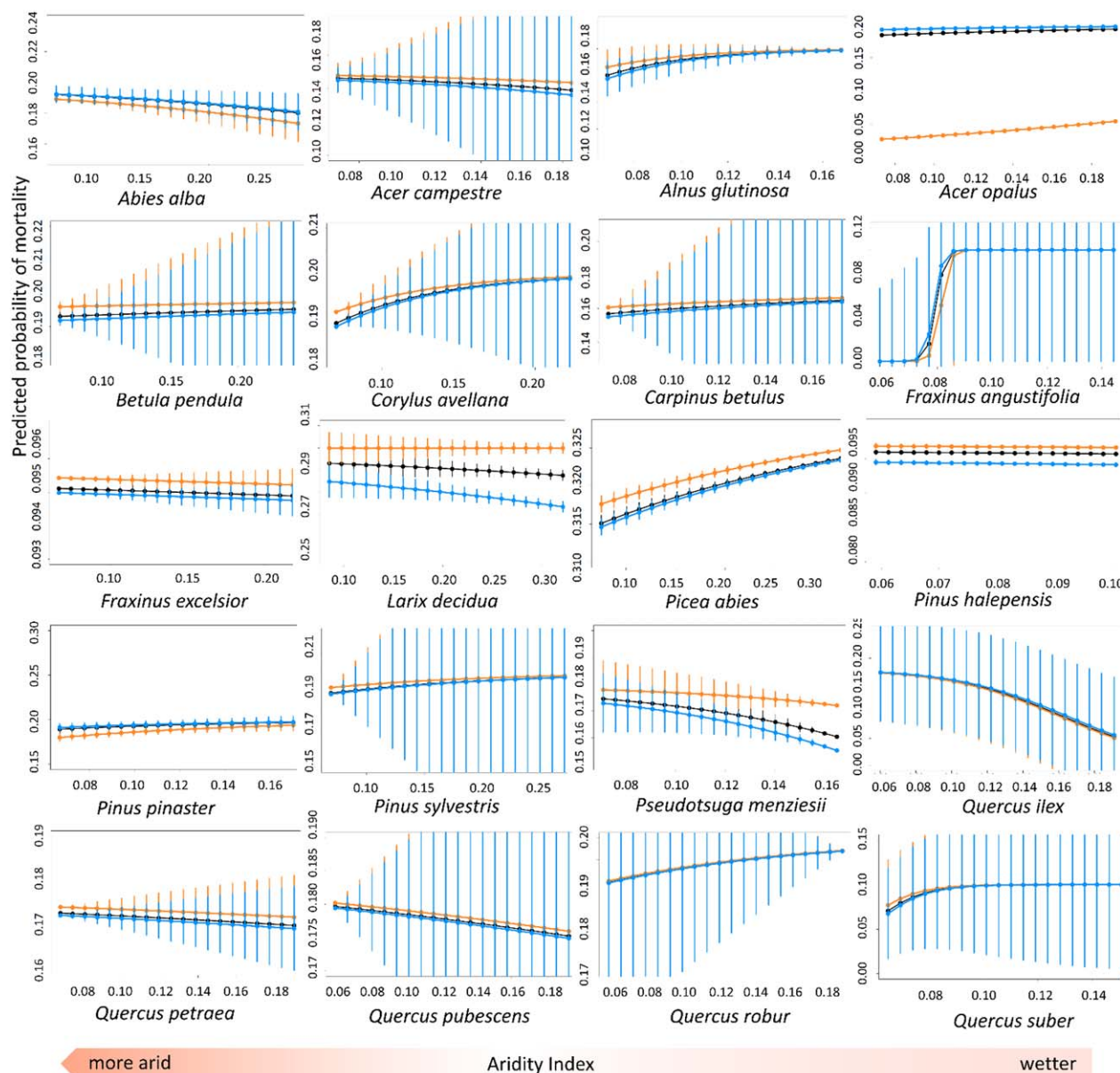


**FIGURE 3** Predicted probability of mortality along an aridity gradient (aridity index = mean annual precipitation/mean annual potential evapotranspiration) for those species showing a significant effect of the modelled hydraulic safety margin (HSM) and/or of the interaction between the modelled HSM and aridity index, according to negative binomial hurdle models. Black, orange and blue lines represent the probability of mortality of populations occurring in areas with average, negative and positive values of HSM along the species distribution ranges, respectively. Note the different scale of the y axis. Confidence intervals, calculated after 100 bootstraps, are shown

## 4 | DISCUSSION

Efforts to understand the vulnerability of forests to drought based on hydraulic traits have been focused at the species level, showing that almost all forest biomes operate with positive but narrow hydraulic safety margins (Choat et al., 2012; Figure 1b). However, here we show that our modelled HSM presents large variability within species ranges, which means that most species have at least one population with a negative hydraulic safety margin (Figure 2). We also show a significant legacy of water deficit in mortality in those populations living with a negative modelled HSM for 15 out of 25 species (Supporting Information Table S3; Figure 3), confirming the significant link between tree

mortality and hydraulic traits (resistance to embolism and HSM) found at the species level (Anderegg et al., 2016).

### 4.1 | The hydraulic safety margin across species

The SWP measured at the lowest quartile of the distribution range of each species ( $\Psi_{\min}$ ) represents the most difficult condition in terms of water availability that the species suffered during the previous 30 years (1979–2010). Here, and in agreement with previous studies, we find a significant positive correlation between the threshold of hydraulic failure ( $\Psi_{50/88}$ ) and  $\Psi_{\min}$  (Figure 1a; Choat et al., 2012; Maherali et al., 2004). However, we also find a significantly negative relationship



between the species-specific modelled HSM and the aridity index, showing that species inhabiting more arid environments present higher modelled HSM than those inhabiting wetter ones (Figure 1b). This result contrasts with the findings of Choat et al. (2012), who found that HSM did not significantly vary across environmental gradients and between biomes (Choat et al., 2012). We explain this discrepancy in terms of differences in the method of estimating  $\Psi_{\min}$  between these studies. In the study by Choat et al. (2012),  $\Psi_{\min}$  was obtained from plants in field conditions, which did not always represent the driest extreme of the species distribution ranges, whereas we modelled  $\Psi_{\min}$  as the soil water potential located in the driest quartile of the species distribution. Furthermore, the results of performing a linear regression between the  $\Psi_{\min}$  values of the 22 species that were included in both studies showed that the slope was not equal to one (i.e., an absolute match between data;  $\Psi_{\min-c} = 0.85 + 0.34\Psi_{\min-swp}$ ;  $p = .01$ ; where  $\Psi_{\min-c}$  comes from Choat et al., 2012 and  $\Psi_{\min-swp}$  is the one calculated in our study; Supporting Information Figure S2). This suggests that our modelled soil water potential data might overestimate the actual  $\Psi_{\min}$  of species at low soil moisture contents because of the exponential nature of soil moisture curves (Supporting Information Figure S1). Further measurements of the minimum water potential of plants in field conditions at the driest margin of species ranges would help to clarify the differences between the studies.

## 4.2 | Identifying plots with a negative hydraulic safety margin

As modelled HSM varies markedly within species distribution ranges, we can identify those populations with negative values of modelled HSM that are likely to be at highest risk of hydraulic failure. We show that all species except *A. pinsapo* and *P. cembra* present populations with a negative hydraulic safety margin (Figure 2). It is likely that we did not detect populations with negative modelled HSM for these two species because of the low number of populations recorded in the Spanish and French NFIs. Indeed, *A. pinsapo* featured only a few scarce populations in South Spain (Farjon, 1990; Vidakovic, 1991), whereas European natural populations of *P. cembra* extend from the subalpine zone of the French Alps and reach the mountainous areas of Ukraine (Ulber, Gugerli, & Bozic, 2004; Supporting Information Table S2), and these areas were not considered in our analysis. In contrast, *P. alba* and *P. hispanica* were the only species with > 50% of their populations having already experienced a negative hydraulic safety margin (Supporting Information Table S2). *Populus alba* mainly occurs in riparian areas, in which the availability of water from the phreatic layer can help to mitigate the negative effect of drought (Blanco Castro, Casado Gonzalez, & Costa Tenorio, 1997). *Platanus hispanica*, a hybrid of *Platanus orientalis* and *P. occidentalis*, has been widely planted in public areas, boundary roads and river banks in Southern Europe (Blanco Castro et al., 1997), and the few populations recorded in the NFIs may also be present in areas with more moderate water availability.

The finding that almost all the species analysed here present populations with negative and/or positive but narrow hydraulic safety margins, suggests that, in the drier conditions projected by the IPCC (2014)

for Western Europe, climate change will be likely to push some populations of these species outside their HSM (Figure 2).

## 4.3 | The legacy of water deficit in plots having experienced a negative hydraulic safety margin

Supporting our initial hypothesis, we detected a fingerprint of water deficit on the mortality of populations with a negative modelled HSM for 15 out of 25 European species for which hurdle models were practicable. For these 15 species, populations having experienced negative modelled HSM showed higher tree mortality than those having experienced positive modelled HSM. These results agree with those of previous works reporting forest dieback in Europe. All species suffering from forest dieback were also detected by our analysis, showing higher mortality in populations with negative modelled HSM than in those with positive modelled HSM (*P. sylvestris*, *Q. suber*, *P. abies* and several unidentified Mediterranean conifers; see Allen et al., 2010, and references therein).

For five of the remaining study species, we found the opposite pattern; populations having experienced negative significant modelled HSM showed less mortality than those having experienced positive HSM (Figure 3; *A. alba*, *A. opalus*, *F. angustifolia*, *P. pinaster* and *Q. ilex*). All of them except *A. alba* are Mediterranean species with a wider distribution than that considered in our study, including populations in North Africa, where more negative HSM are expected. The importance of the modelled HSM in *A. alba* mortality is very low (estimate = 0.03; Supporting Information Table S3) in comparison with other variables (competition and aridity index have estimate values of 0.53 and -0.77, respectively; Supporting Information Table S3), so although it is significant, this result needs to be considered with caution. Furthermore, *F. angustifolia*, like *P. alba*, is a riparian tree, and any effect of drought can be mitigated by the availability of phreatic water (Blanco Castro et al., 1997). In the case of *Q. ilex*, the Spanish populations of this species have been severely affected by the fungus *Phytophthora cinnamomi* (Corcobado, Cubera, Juárez, Moreno, & Solla, 2014), and some signs of the plague can remain in our data, despite the efforts made to clean our dataset from confounding factors.

For the other five species analysed (*Arbutus unedo*, *I. aquifolium*, *Pinus nigra*, *Populus tremula* and *P. uncinata*), no significant relationship between modelled HSM and the amount of mortality predicted was found. Again, in some of these cases, the lack of a footprint of long-term water deficit on the average mortality in populations with negative modelled HSM can be explained by the fact that the distributions derived from the NFI from Spain and France do not cover the entire distribution range of all of the species. This is particularly the case for the driest edge of the distribution range of those species also found in North Africa (*A. unedo*) and Turkey (*P. nigra*). Also, little differences between populations can hide any effect of modelled HSM on tree mortality (see estimates values for each factor in Supporting Information Table S3). For all these species, other factors, rather than modelled HSM, must be modulating tree mortality. Indeed, climatic variables (including aridity) and competition seem to be drivers of tree mortality, even considering the modulation exerted by the hydraulic traits (HSM).



Our results support previous analysis showing that drought-induced tree mortality increases at the driest part of the species distribution ranges (Anderegg et al., 2015; Young et al., 2017; Figure 3) and that this phenomenon is also controlled by competition (Ruiz-Benito et al., 2013). *Abies alba*, *A. campestris*, *A. opalus*, *F. excelsior*, *L. decidua*, *P. halepensis*, *Q. ilex*, *Q. petraea* and *Q. pubescens* (Supporting Information Table S3) showed higher mortality at the drier locations, suggesting the vulnerability of these populations to increasingly frequent droughts at the drier edge of their distribution. In contrast, *Q. suber* showed lower mortality at the drier locations, but this is probably attributable to the lack of the driest Moroccan populations in our analysis.

#### 4.4 | Final remarks and further work

Our approach assumes that the within-species phenotypic variability in  $\Psi_{50/88}$  is negligible (Anderegg, 2015; Hajek, Kurjak, von Wühlisch, Delzon, & Schuldt, 2016; Lamy et al., 2014; Sáenz-Romero et al., 2013), but this would not be the case for all species. In general, intra-specific variability of  $\Psi_{50/88}$  has been shown to be lower than that found across species (Anderegg, 2015). But, although low variability in  $\Psi_{50}$  was found for most of the conifers (Anderegg, 2015; Lamy et al., 2014; Martínez-Vilalta et al., 2009; Sáenz-Romero et al., 2013; Wortemann et al., 2011), recent studies reflecting some within-species variability in embolism resistance have recently been reported (David-Schwartz et al., 2016; López et al., 2013, 2016). These studies show that marginal populations of *Pinus canariensis* and *P. halepensis* present slightly more negative resistance to embolism than populations at the core of the species ranges. In particular, for the xeric species *P. canariensis*, only the driest populations showed plasticity in embolism resistance (López et al., 2013, 2016). Overall, more phenotypic variation in  $\Psi_{50/88}$  has been reported for angiosperms than for gymnosperms (Anderegg, 2015; Schuldt et al., 2016). Further studies evaluating the intraspecific variability in hydraulic traits are needed to clarify the lack of a footprint of water deficit in populations with negative modelled HSM found here for some species.

#### DATA ACCESSIBILITY

Individual tree data from National Forest Inventories of Spain and France are freely available at <http://www.mapama.gob.es/es/desarrollo-rural/temas/politica-forestal/inventario-cartografia/inventario-forestal-nacional/> and <http://inventaire-forestier.ign.fr/spip/>, respectively. The resistance to embolism dataset is published, in part, by Choat et al. (2012).

#### ACKNOWLEDGMENTS

For this study, the authors received financial support from the program Investments for the Future IDEX Bordeaux (ANR-10-IDEX-03-02) and EQUIPEX (ANR-10-EQPX-16, XYLOFOREST) from the French National Agency for Research. N.G.M. was supported by the Agreenskills+ fellowship programme, which has received funding from the European Union's Seventh Framework Programme under grant agreement No. FP7-26719 (Agreenskills+ contract). We are

very grateful to Natalia Vízcaíno Palomar for advising us on the statistical analysis. We are grateful to the Royal Botanic Gardens, Kew and the National Pinetum of Bedgebury for permission to collect samples.

#### REFERENCES

- Allen, C. D., Breshears, D. D., & McDowell, N. G. (2015). On underestimation of global vulnerability to tree mortality and forest die-off from hotter drought in the Anthropocene. *Ecosphere*, 6, art129.
- Allen, C. D., Macalady, A. K., Chenchouni, H., Bachelet, D., McDowell, N., Vennetier, M., ... Cobb, N. (2010). A global overview of drought and heat-induced tree mortality reveals emerging climate change risks for forests. *Forest Ecology and Management*, 259, 660–684.
- Anderegg, W. R. L. (2015). Spatial and temporal variation on plant hydraulic traits and their relevance for climate change impacts on vegetation. *New Phytologist*, 205, 1008–1014.
- Anderegg, W. R. L., Flint, A., Huang, C., Flint, L., Berry, J. A., Davis, F. W., ... Field, C. B. (2015). Tree mortality predicted from drought-induced vascular damage. *Nature Geoscience*, 8, 367–371.
- Anderegg, W. R. L., Klein, T., Bartlett, M., Sack, L., Pellegrini, A. F. A., Choat, B., & Jansen, S. (2016). Meta-analysis reveals that hydraulic traits explain cross-species patterns of drought-induced tree mortality across the globe. *Proceedings of the National Academy of Sciences USA*, 113, 5024–5029.
- Balsamo, G., Albergel, C., Beljaars, A., Boussetta, S., Brun, E., Cloke, H., ... Vitart, F. (2015). ERA-Interim/Land: A global land surface reanalysis data set. *Hydrology and Earth System Sciences*, 19, 389–407.
- Barigah, T. S., Charrier, O., Douris, M., Bonhomme, M., Herbette, S., Améglio, T., ... Cochard, H. (2013). Water stress-induced xylem hydraulic failure is a causal factor of tree mortality in beech and poplar. *Annals of Botany*, 112, 1431–1437.
- Benito-Garzón, M., & Fernandez-Manjarrés, J. F. (2015). Testing scenarios for assisted migration of forest trees in Europe. *New Forests*, 46, 979–994.
- Benito-Garzón, M., Ruiz-Benito, P., & Zavala, M. A. (2013). Inter-specific differences in tree growth and mortality responses to environmental drivers determine potential species distribution limits in Iberian forests. *Global Ecology and Biogeography*, 22, 1141–1151.
- Berdanier, A. B., & Clark, J. S. (2016). Multiyear drought-induced morbidity preceding tree death in southeastern U.S. forests. *Ecological Applications*, 26, 17–23.
- Blanco Castro, E., Casado Gonzalez, M., & Costa Tenorio, M. (1997). *Los bosques Ibericos: Una interpretacion geobotanica* (p. 557). Barcelona, Planeta.
- Bonan, G. B. (2008). Forests and climate change: Forcings, feedbacks, and the climate benefits of forests. *Science*, 320, 1444–1449.
- Bouche, P. S., Larter, M., Domec, J.-C., Burtlett, R., Gasson, P., Jansen, S., & Delzon, S. (2014). A broad survey of hydraulic and mechanical safety in the xylem of conifers. *Journal of Experimental Botany*, 65, 4419–4431.
- Brodribb, T., & Hill, R. S. (1999). The importance of xylem constraints in the distribution of conifer species. *New Phytologist*, 143, 365–372.
- Brodribb, T. J., & Cochard, H. (2009). Hydraulic failure defines the recovery and point of death in water-stressed conifers. *Plant Physiology*, 149, 575–584.
- Brodribb, T. J., Bowman, D. J. M. S., Nichols, S., Delzon, S., & Burtlett, R. (2010). Xylem function and growth rate interact to determine recovery rates after exposure to extreme water deficit. *New Phytologist*, 188, 533–542.

- Campbell, G. S. (1985). *Soil physics with basic; Transport models for soil-plant systems*. Amsterdam: Elsevier.
- Choat, B., Badel, E., Burtlett, R., Delzon, S., Cochard, H., & Jansen, S. (2016). Noninvasive measurement of vulnerability to drought-induced embolism by X-Ray microtomography. *Plant Physiology*, 170, 273–282.
- Choat, B., Jansen, S., Brodribb, T. J., Cochard, H., Delzon, S., Bhaskar, R., ... Zanne, A. E. (2012). Global convergence in the vulnerability of forests to drought. *Nature*, 491, 752–755.
- Clark, J. S., Iverson, L., Woodall, C. W., Allen, C. D., Bell, D. M., Bragg, D. C., ... Zimmermann, N. E. (2016). The impacts of increasing drought on forest dynamics, structure, and biodiversity in the United States. *Global Change Biology*, 22, 2329–2352.
- Cochard, H., Badel, E., Herbette, S., Delzon, S., Choat, B., & Jansen, S. (2013). Methods for measuring plant vulnerability to cavitation: A critical review. *Journal of Experimental Botany*, 64, 4779–4791.
- Cochard, H., Delzon, S., & Badel, E. (2015). X-ray microtomography (micro-CT): A reference technology for high-resolution quantification of xylem embolism in trees. *Plant, Cell and Environment*, 38, 201–206.
- Corcobado, T., Cubera, E., Juárez, E., Moreno, G., & Solla, A. (2014). Drought events determine performance of *Quercus ilex* seedlings and increase their susceptibility to *Phytophthora cinnamomi*. *Agricultural and Forest Meteorology*, 192–193, 1–8.
- David-Schwartz, R., Paudel, I., Mizrahi, M., Delzon, S., Cochard, H., Lukyanov, V., ... Cohen, S. (2016). Indirect evidence for genetic differentiation in vulnerability to embolism in *Pinus halepensis*. *Frontiers in Plant Science*, 7, 768.
- Dee, D. P., Uppala, S. M., Simmons, A. J., Berrisford, P., Poli, P., Kobayashi, S., ... Vitart, F. (2011). The ERA-Interim reanalysis: Configuration and performance of the data assimilation system. *Quarterly Journal of the Royal Meteorological Society*, 137, 553–597.
- Delzon, S., & Cochard, H. (2014). Recent advances in tree hydraulics highlight the ecological significance of the hydraulic safety margin. *New Phytologist*, 203, 355–358.
- Delzon, S., Douthe, C., Sala, A., & Cochard, H. (2010). Mechanism of water-stress induced cavitation in conifers: Bordered pit structure and function support the hypothesis of seal capillary-seeding. *Plant, Cell and Environment*, 33, 2101–2111.
- Domec, J.-C., & Gartner, B. L. (2001). Cavitation and water storage capacity in bole xylem segments of mature and young Douglas-fir trees. *Trees*, 15, 204–214.
- Engelbrecht, B. M. J. (2012). Plant ecology: Forests on the brink. *Nature*, 491, 675.
- Farjon, A. (1990). *Pinaceae: Drawings and descriptions of the genera Abies, Cedrus, Pseudolarix, Keteleeria, Nothotsuga, Tsuga, Cathaya, Pseudotsuga, Larix and Picea*. Königstein, Germany: Koeltz Scientific Books.
- Gómez-Aparicio, L., García-Valdés, R., Ruiz-Benito, P., & Zavala, M. A. (2011). Disentangling the relative importance of climate, size and competition on tree growth in Iberian forests: Implications for forest management under global change. *Global Change Biology*, 17, 2400–2414.
- Hajek, P., Kurjak, D., von Wühlisch, G., Delzon, S., & Schuldt, B. (2016). Intraspecific variation in wood anatomical, hydraulic, and foliar traits in ten European beech provenances differing in growth yield. *Frontiers in Plant Science*, 7, 791.
- Hartmann, H., Adams, H. D., Anderegg, W. R. L., Jansen, S., & Zeppel, M. J. B. (2015). Research frontiers in drought-induced tree mortality: Crossing scales and disciplines. *New Phytologist*, 205, 965–969.
- Hartmann, H., Ziegler, W., Kolle, O., & Trumbore, S. (2013). Thirst beats hunger – Declining hydration during drought prevents carbon starvation in Norway spruce saplings. *New Phytologist*, 200, 340–349.
- Herbette, S., Wortemann, R., Awad, H., Huc, R., Cochard, H., & Barigah, T. S. (2010). Insights into xylem vulnerability to cavitation in *Fagus sylvatica* L.: Phenotypic and environmental sources of variability. *Tree Physiology*, 30, 1448–1455.
- Hijmans, R., Cameron, S., Parra, J., Jones, P., & Jarvis, A. (2005). Very high resolution interpolated climate surfaces for global land areas. *International Journal of Climatology*, 25, 1965–1978.
- IPCC. (2014). Climate change 2014 synthesis report. In R. K. Pachauri & L. A. Meyer (Eds.), *Contribution of working groups I, II and III to the fifth assessment report of the intergovernmental panel on climate change* (p. 151). Geneva, Switzerland: IPCC.
- Kunstler, G., Falster, D., Coomes, D. A., Hui, F., Kooyman, R. M., Laughlin, D. C., ... Westoby, M. (2016). Plant functional traits have globally consistent effects on competition. *Nature*, 529, 204–207.
- Lamy, J.-B., Delzon, S., Bouche, P. S., Alia, R., Vendramin, G. G., Cochard, H., & Plomion, C. (2014). Limited genetic variability and phenotypic plasticity detected for cavitation resistance in a Mediterranean pine. *New Phytologist*, 201, 874–886.
- Lens, F., Picon-Cochard, C., & Delmas, C. E. L. (2016). Herbaceous angiosperms are not more vulnerable to drought-induced embolism than angiosperm trees. *Plant Physiology*, 172, 661–667.
- Lens, F., Tixier, A., Cochard, H., Sperry, J. S., Jansen, S., & Herbette, S. (2013). Embolism resistance as a key mechanism to understand adaptive plant strategies. *Current Opinion in Plant Biology*, 16, 287–292.
- Linares, J. C., & Camarero, J. J. (2011). Growth patterns and sensitivity to climate predict silver fir decline in the Spanish Pyrenees. *European Journal of Forest Research*, 131, 1001–1012.
- López, R., Cano, F. J., Choat, B., Cochard, H., & Gil, L. (2016). Plasticity in vulnerability to cavitation of *Pinus canariensis* occurs only at the driest end of an aridity gradient. *Frontiers in Plant Science*, 7, 769.
- López, R., López de Heredia, U., Collada, C., Cano, F. J., Emerson, B. C., Cochard, H., & Gil, L. (2013). Vulnerability to cavitation, hydraulic efficiency, growth and survival in an insular pine (*Pinus canariensis*). *Annals of Botany*, 111, 1167–1179.
- Maherali, H., Pockman, W. T., & Jackson, R. B. (2004). Adaptive variation in the vulnerability of woody plants to xylem cavitation. *Ecology*, 85, 2184–2199.
- Martínez-Vilalta, J., Cochard, H., Mencuccini, M., Sterck, F., Herrero, A., Korhonen, J. F. J., ... Zweifel, R. (2009). Hydraulic adjustment of Scots pine across Europe. *New Phytologist*, 184, 353–364.
- McDowell, N., Pockman, W. T., Allen, C. D., Breshears, D. D., Cobb, N., Kolb, T., ... Yepez, E. A. (2008). Mechanisms of plant survival and mortality during drought: Why do some plants survive while others succumb to drought? *New Phytologist*, 178, 719–739.
- Meinzer, F. C., Johnson, D. M., Lachenbruch, B., McCulloh, K. A., & Woodruff, D. R. (2009). Xylem hydraulic safety margins in woody plants: Coordination of stomatal control of xylem tension with hydraulic capacitance. *Functional Ecology*, 23, 922–930.
- Neumann, M., Mues, V., Moreno, A., Hasenauer, H., & Seidl, R. (2017). Climate variability drives recent tree mortality in Europe. *Global Change Biology*, 23, 4788–4797.
- Pammenter, N. W., & Vander Willigen, C. (1998). A mathematical and statistical analysis of the curves illustrating vulnerability of xylem to cavitation. *Tree Physiology*, 18, 589–593.
- Panagos, P., Van Liedekerke, M., Jones, A., & Montarella, L. (2012). European soil data centre: response to European policy support and public data requirements. *Land Use Policy*, 29, 329–338.
- Peng, C., Ma, Z., Lei, X., Zhu, Q., Chen, H., Wang, W., ... Zhou, X. (2011). A drought-induced pervasive increase in tree mortality across Canada's boreal forests. *Nature Climate Change*, 1, 467–471.

- Phillips, O. L., Aragão, L. E. O. C., Lewis, S. L., Fisher, J. B., Lloyd, J., López-González, G., ... Torres-Lezama, A. (2009). Drought sensitivity of the Amazon rainforest. *Science*, 323, 1344–1347.
- Purves, D. W. (2009). The demography of range boundaries versus range cores in eastern US tree species. *Proceedings of the Royal Society B: Biological Sciences*, 276, 1477–1484.
- R Development Core Team. (2016). *R: A language and environment for statistical computing*. Vienna, Austria: R Foundation for Statistical Computing. Retrieved from <http://www.R-project.org>
- Ruiz-Benito, P., Lines, E. R., Gómez-Aparicio, L., Zavala, M. A., & Coomes, D. A. (2013). Patterns and drivers of tree mortality in Iberian forests: Climatic effects are modified by competition. *PLoS One*, 8, e56843.
- Sáenz-Romero, C., Lamy, J.-B., Loya-Rebollar, E., Plaza-Aguilar, A., Burlett, R., Lobit, P., & Delzon, S. (2013). Genetic variation of drought-induced cavitation resistance among *Pinus hartwegii* populations from an altitudinal gradient. *Acta Physiologiae Plantarum*, 35, 2905–2913.
- Schuldt, B., Knutzen, F., Delzon, S., Jansen, S., Müller-Haubold, H., Burlett, R., ... Leuschner, C. (2016). How adaptable is the hydraulic system of European beech in the face of climate change-related precipitation reduction? *New Phytologist*, 210, 443–458.
- Sperry, J. S., Adler, F. R., Campbell, G. S., & Comstock, J. P. (1998). Limitation of plant water use by rhizosphere and xylem conductance: Results from a model. *Plant, Cell and Environment*, 21, 347–359.
- Stahl, U., Reu, B., & Wirth, C. (2014). Predicting species' range limits from functional traits for the tree flora of North America. *Proceedings of the National Academy of Sciences USA*, 111, 13739–13744.
- Steinkamp, J., & Hickler, T. (2015). Is drought-induced forest dieback globally increasing? *Journal of Ecology*, 103, 31–43.
- Torres-Ruiz, J. M., Cochard, H., Choat, B., Jansen, S., López, R., Tomášková, I., ... Delzon, S. (2017). Xylem resistance to embolism: Presenting a simple diagnostic test for the open vessel artefact. *New Phytologist*, 215, 489–499.
- Torres-Ruiz, J. M., Jansen, S., Choat, B., McElrone, A. J., Cochard, H., Brodribb, T. J., ... Delzon, S. (2014). Direct X-ray microtomography observation confirms the induction of embolism upon xylem cutting under tension. *Plant Physiology*, 167, 40.
- Tyree, M. T. (1999). Refilling of embolized vessels in young stems of laurel. Do we need a new paradigm? *Plant Physiology*, 120, 11–22.
- Ulber, M., Gugerli, F., & Bozic, G. (2004). *EUFORGEN technical guidelines for genetic conservation and use for Swiss stone pine (Pinus cembra)* (p. 6). Rome: Bioversity International.
- Urli, M., Lamy, J.-B., Sin, F., Burlett, R., Delzon, S., & Porté, A. J. (2015). The high vulnerability of *Quercus robur* to drought at its southern margin paves the way for *Quercus ilex*. *Plant Ecology*, 216, 177–187.
- Urli, M., Porté, A. J., Cochard, H., Guengant, Y., Burlett, R., & Delzon, S. (2013). Xylem embolism threshold for catastrophic hydraulic failure in angiosperm trees. *Tree Physiology*, 33, 672–683.
- van Mantgem, P. J., Stephenson, N. L., Byrne, J. C., Daniels, L. D., Franklin, J. F., Fulé, P. Z., ... Veblen, T. T. (2009). Widespread increase of tree mortality rates in the western United States. *Science*, 323, 521–524.
- Vanderwel, M. C., Lyutsarev, V. S., & Purves, D. W. (2013). Climate-related variation in mortality and recruitment determine regional forest-type distributions. *Global Ecology and Biogeography*, 22, 1192–1203.
- Vidakovic, M. (1991). *Conifers: Morphology and variation* [Translated from Croatian by Maja Soljan]. Croatia: Graficki Zavod Hrvatske.
- Wortemann, R., Herbette, S., Barigah, T. S., Fumanal, B., Alia, R., Ducousso, A., ... Cochard, H. (2011). Genotypic variability and phenotypic plasticity of cavitation resistance in *Fagus sylvatica* L. across Europe. *Tree Physiology*, 31, 1175–1182.
- Young, D. J. N., Stevens, J. T., Earles, J. M., Moore, J., Ellis, A., Jirka, A. L., & Latimer, A. M. (2017). Long-term climate and competition explain forest mortality patterns under extreme drought. *Ecology Letters*, 20, 78–86.

## BIOSKETCH

The authors' research is focused on forest ecology and global change, with expertise ranging from ecophysiology, genetics, ecological modelling to remote sensing. The authors use multidisciplinary approaches to understand complex processes in ecology, which provide new innovative approaches to study global changes in vegetation.

## SUPPORTING INFORMATION

Additional Supporting Information may be found online in the supporting information tab for this article.

**How to cite this article:** Benito Garzón M, González Muñoz N, Wigneron J-P, Moisy C, Fernández-Manjarrés J, Delzon S. The legacy of water deficit on populations having experienced negative hydraulic safety margin. *Global Ecol Biogeogr*. 2017;00:1–11. <https://doi.org/10.1111/geb.12701>